ELSEVIER

Journal of Chromatography A, 891 (2000) 139–148

JOURNAL OF CHROMATOGRAPHY A

www.elsevier.com/locate/chroma

Simple interface for capillary electrophoresis–inductively coupled plasma atomic emission spectrometry

Biyang Deng, Wing-Tat Chan*

Department of Chemistry, University of Hong Kong, Pokfulam Road, Hong Kong, China

Received 9 February 2000; received in revised form 4 May 2000; accepted 25 May 2000

Abstract

A simple interface has been developed to couple capillary electrophoresis (CE) to inductively coupled plasma atomic emission spectrometry (ICP-AES) for metal speciation. A concentric glass nebulizer with elongated tip is used as the CE–ICP interface. The CE capillary is the central tube of the nebulizer. A platinum wire is wrapped across the exit end of the CE capillary to provide electrical connection to the CE power supply. No sheath flow of buffer solution is needed. A simple cooling system has also been developed. A peristaltic pump circulates water through a plastic tube that encloses the section of the CE capillary between the CE instrument and the ICP spectrometer. Characteristics of the CE–ICP interface, e.g., elution time, nebulization and transport efficiency and peak broadening, versus carrier gas flow-rate have been studied. Comparisons to a previous design with the Pt electrode inserted into the end of the CE capillary are made where appropriate. The reproducibility (RSD) in ICP emission intensity of the system is <4%. Detection limits of Cr and Cu are ~5 ng/ml.

Keywords: Interfaces, CE–ICP; Detection, electrophoresis; Instrumentation; Metal cations; Metal complexes; Inorganic anions

1. Introduction

Capillary electrophoresis (CE) is a powerful yet relatively simple separation technique for a wide range of samples in environmental, biological and clinical analysis [1–5]. The hyphenated technique to couple CE to inductively coupled plasma (ICP) spectrometry for elemental speciation further broadens the range of CE applications [6–22]. The design of the CE–ICP interface is critical to the analytical performance of CE–ICP [23]. Interfaces based on glass concentric [6,7,12,20], high efficiency [19], direct injection [9], glass frit [8], ultrasonic [11], and microconcentric nebulizers [15,16,18,21], and hydride generation [14,22] have been reported.

A CE–ICP interface based on a concentric nebulizer has been reported by this research group [24]. The central capillary of the nebulizer is replaced by the CE capillary. A Pt wire was inserted into the CE capillary for electrical connection. A major advantage of the CE–ICP interface is that it operates without the need of a sheath buffer flow. A sheath buffer flow adds to the complexity of CE–ICP operation and may introduce further peak broadening due to the liquid flow.

Using the CE–ICP interface, baseline separation

*Corresponding author. Tel.: +852-2859-2156; fax: +852-2857-1586.

E-mail address: wtchan@hkusua.hku.hk (W.-T. Chan).

0021-9673/00/$ – see front matter
PII: S0021-9673(00)00622-1

of Cr^{3+} and $Cr_2O_7^{2-}$ was achieved with detection limits of $8 \cdot 10^{-12}$ g Cr [24]. The interface, however, is mechanically unstable because the thin Pt electrode (diameter=25 μm) can wiggle freely inside the CE capillary. Furthermore, the portion of the CE capillary between the CE instrument and the CE–ICP interface was exposed to air and no active cooling was implemented. Temperature of the capillary increases during a CE run and may vary from run to run. Temperature fluctuation is especially severe for CE–ICP because the high-temperature ICP source increases the temperature of the environment. Long term stability of the CE–ICP system suffers.

In this work, the CE–ICP interface is further developed with a new electrode configuration and a novel cooling system to improve its long-term stability. The experimental set-up of the CE–ICP-atomic emission spectrometry (AES) interface is described. The characteristics of the interface will be discussed and compared to the previous design. Analytical figures of merit in terms of reproducibility and detection limits are also presented.

2. Experimental

A commercial CE instrument and multi-channel ICP-AES spectrometer were used to reduce the development time of the CE–ICP system. The general experimental set-up has been described previously [24]. New developments and major equipment are summarized below.

2.1. Capillary electrophoresis

The original on-column UV detector of the CE instrument (Biofocus 2000, Bio-Rad, Hercules, CA, USA) was disabled. An ICP spectrometer was used instead to determine multiple metal species simultaneously. The exit section of the CE capillary was placed inside the custom-made nebulizer (see Section 2.3 for details) for aerosol generation and analyte transport to the ICP spectrometer. Typical CE voltage and current were 15 kV and 15 μA, respectively.

Fused-silica CE capillaries (Polymicro Technology, Phoenix, AZ, USA) with inner diameters of 75 and 100 μm and outer diameters of 363 μm were used. The length of the capillaries was 100 to 150 cm.

2.2. Inductively coupled plasma atomic emission spectrometer

An Echelle grating ICP-AES system (Plasmaquant 110, Carl Zeiss, Jena, Germany) was used. The ICP forward power was 1.0 kW. Outer and intermediate gas flow-rates were 12 and 0.8 l/min, respectively. Carrier gas flow-rate was 0.6 to 1.2 l/min. The observation height was 10 mm above the load coil. Temporal ICP emission intensity of Cr II 266.7 nm, Cu I 324.7 nm, and Mn II 260.6 nm were measured at a sampling rate of 3 s per data point over a CE run.

2.3. CE–ICP interface

The basic design of the CE–ICP interface has been reported previously [24]. A glass concentric nebulizer was used as the CE–ICP interface (Fig. 1). The CE capillary is the central capillary of the nebulizer. The end of the outer tube of the nebulizer is shaped as a cylindrical tube (length ~0.5 cm, inner diameter 0.5 mm) so that uncertainty in the position of the central capillary does not effect the nebulization efficiency significantly [24].

A major change in the new CE–ICP interface is that the Pt electrode is not inserted into the CE capillary. Instead, a 0.5 cm section of a platinum wire (diameter=50 μm and total length=10 cm) was wrapped across the opening of the outlet end of the CE capillary for electrical connection to the CE high-voltage power supply (Fig. 1). The wire was fixed in position with a thin coat of epoxy round the end of the capillary. The glued section of the CE capillary and Pt wire is threaded through a small hole that was punched on a septum (Puresep-T septa, diameter 6 mm and thickness 3 mm, Cole-Parmer, Vernon Hills, IL, USA). The septum was held at the end of the nebulizer with a PTFE reducer type connector (Cole-Parmer). One end of the PTFE connector (inner diameter 1.6 mm) was sealed by the septum and the other end (inner diameter 6 mm) was connected to the nebulizer. The PTFE connector was

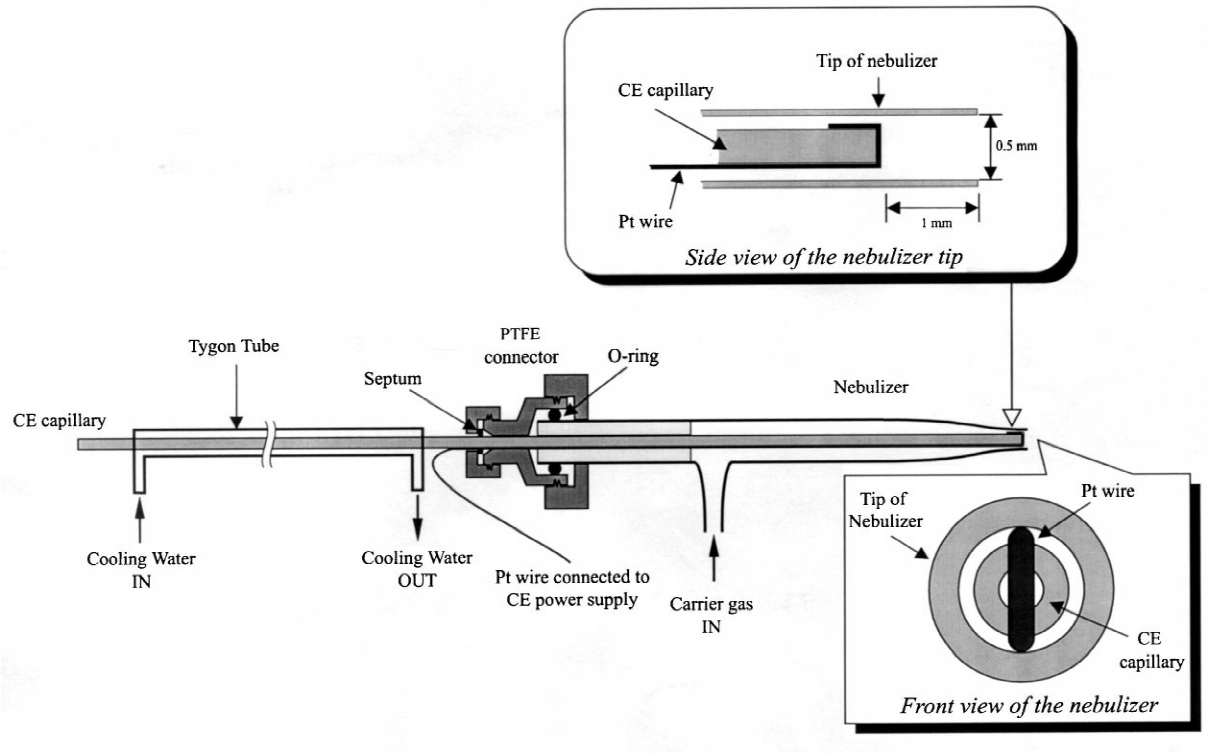

Fig. 1. Schematic diagram of the CE–ICP interface.

fixed to the nebulizer so that the CE capillary was placed at a position of 1 mm from the tip of the nebulizer.

The CE capillary inside the capillary cartridge of the CE instrument (~30 cm in length) was water-cooled by the CE instrument's cooling system. The portion of CE capillary connecting the nebulizer to the CE instrument (~110 cm long for a 150 cm capillary), however, is exposed to air and the temperature of the capillary increases during electrophoresis. To reduce thermal effects on analyte migration, the aforementioned portion of the capillary was inserted into a plastic tube (Tygon R-3603, Cole-Parmer) and was cooled by circulating water (20°C) with a peristaltic pump through the tube.

Sample was introduced into the CE capillary using hydrodynamic injection. A nitrogen gas pressure of 5 p.s.i. was used to inject the sample solution into the capillary (1 p.s.i.=6894.76 Pa). For a capillary of 150 cm×100 μm I.D., sample volume of an aqueous solution is ~0.8 μl for a 10 s injection period. The sample volume is approximately 7% of the total capillary volume. During sample injection, the Ar carrier gas flow was stopped to prevent air from entering the CE capillary.

A stream of Ar carrier gas was used to draw the CE electrolyte through the CE capillary and nebulize the solution into fine aerosol. Since the carrier gas flow determines the electrolyte flow-rate inside the capillary and thus the analyte elution time, the carrier gas flow-rate must be controlled tightly. The gas flow-rate through the CE–ICP interface was adjusted with a needle valve and continuously monitored using a mass flow meter (SMA1816, Omega Engineering, Stamford, CT, USA) to ensure a constant flow-rate. The gas flow was turned on 5 s after the CE high-voltage power supply was switched on. A locally constructed cylindrical spray chamber (volume ~110 ml) was used to remove large droplets from the spray.

2.4. Chemical reagents

Sodium acetate buffer (0.02 *M*) was prepared from sodium acetate trihydrate (analytical-reagent grade, Beijing Chemical Works, China) and the pH of the buffer electrolyte was adjusted to 5.0 using diluted nitric acid (guaranteed-reagent grade, Merck, Darmstadt, Germany). $K_2Cr_2O_7$ and $CrCl_3 \cdot 6H_2O$ (analytical-reagent grade, Aldrich, Milwaukee, WI, USA), $CuSO_4 \cdot 5H_2O$ (analytical-reagent grade, Beijing Chemical Works), disodium dihydrogen ethylenediaminetetraacetate dihydrate (analytical-reagent grade, Aldrich) were used for sample preparation. The solutions were prepared by dissolving the appropriate amounts of the chemicals in distilled water. The pH of all solutions was adjusted to 5.0 using diluted nitric acid.

3. Results and discussion

Analytical performance of CE–ICP depends critically on the characteristics of the CE–ICP interface. A carrier gas stream is used to nebulize the CE effluent into fine aerosol for transport to the ICP spectrometer. The nebulization and transport efficiency of the interface determines the sensitivity of CE–ICP. The carrier gas flow also produces a pressure difference at the end of the CE capillary. The buffer electrolyte is drawn through the capillary by Bernoulli's principle. The flow pattern of the buffer electrolyte is parabolic and the CE peaks are broadened. To preserve the high-resolution capability of CE, the peak broadening effects of the carrier gas flow must be minimized.

The characteristics of the CE–ICP interface are first examined with the CE voltage turned off, i.e., no separation of analyte by CE occurs. A fixed volume of Cu^{2+} solution was injected into the capillary to simulate the discrete CE sample. Eluted time, peak width, and ICP emission intensity at different carrier gas flow-rate were determined. A relatively large sample volume was used to reduce uncertainty in sample length due to the sample injection process.

3.1. Elution time due to carrier gas flow

A major driving force of the flow of the electrolyte solution in CE–ICP is the carrier gas flow [24]. The electrolyte flow-rate due to the carrier gas flow is comparable to the sum of electroosmotic flow-rate and ion mobility at low gas flow-rate, but exceeds the flows by an order of magnitude at higher gas flow [24]. Elution time of the sample, therefore, depends mainly on the carrier gas flow-rate.

Elution time of the Cu sample plug against carrier gas flow-rate for different configuration of CE–ICP interface is shown in Fig. 2. The CE voltage was switched off, i.e., the elution of Cu is due to the carrier gas flow alone. The CE capillary was first filled with distilled–deionized water and a fixed volume of ~1.6 μl of 500 ng/ml Cu^{2+} solution was injected into the CE capillary. The carrier gas flow was turned off during sample injection. The length of the sample inside the capillary was ~20 cm. The total capillary length was 150 cm. The carrier gas flow was then turned on and the temporal ICP emission intensity of Cu I 324.7 nm was measured. The elution time was defined as the time for the appearance of the center of the Cu peak.

Three configurations of CE–ICP interface are used in Fig. 2. All configurations used the same outer shell of the CE–ICP nebulizer, but the Pt wire electrode was placed at different position. A Pt wire of 50 μm diameter was wrapped across the exit end of the CE capillary, inserted into the CE capillary, or

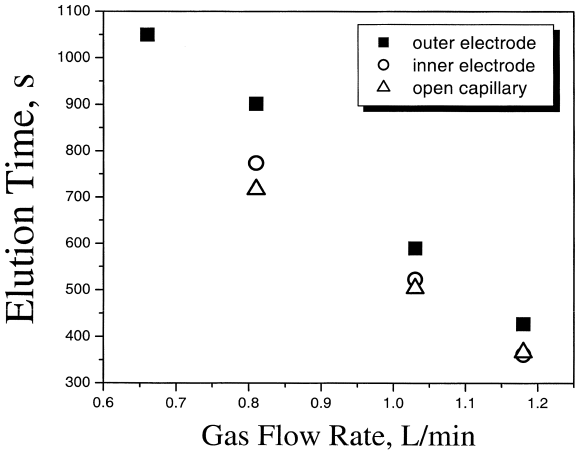

Fig. 2. Elution time of the Cu^{2+} sample plug versus carrier gas flow-rate for different configurations of the CE–ICP interface. CE voltage was not applied.

removed from the interface. The configurations will be called outer electrode, inner electrode, and open capillary configurations, respectively. Elution time reduces as carrier gas flow-rate increases for all CE–ICP configurations. The outer electrode configuration, however, gives longer elution time for the same gas flow-rate. Elution time for the inner electrode is intermediate and the open capillary has the smallest elution time. The trend corresponds to the size of the opening of the CE capillary at the exit end. The Pt wire blocks ~61% and ~25% of the cross sectional area of the CE capillary for outer electrode and inner electrode configurations, respectively. A restricted opening will allow a lower volumetric flow-rate for the same driving force (gas flow-rate).

Since the elution time of the sample is approximately the duration of time that the analytes are separated under the CE electric field during a CE run, the outer electrode configuration potentially gives a higher CE resolution.

For long elution time and thus high CE–ICP resolution, the carrier gas flow-rate should be as low as possible. However, the carrier gas flow-rate must be maintained at certain level for adequate nebulization and transport of aerosols. At a carrier gas flow-rate of 0.66 l/min, a peak is obtained for the Cu sample plug using the outer electrode CE–ICP configuration, but no peak was observed for the inner electrode and open capillary configurations (Fig. 2). A combination of longer elution time and lower operating range of carrier gas flow-rate for the outer electrode configuration, therefore, should give higher CE–ICP resolution compared to other configurations.

3.2. Nebulization and transport efficiency

The integrated ICP emission intensity of Cu I 324.7 nm reduces as carrier gas flow-rates reduces (Fig. 3). Again, a fixed volume of Cu sample was injected into the capillary first. The sample size and concentration were the same as previous section. No CE voltage was applied. The reduced ICP intensity for a fixed sample volume is due to a reduction in nebulization and transport efficiency of the CE–ICP interface at lower gas flow-rate. Similarly, the peak height of Cu emission reduces with gas flow-rate

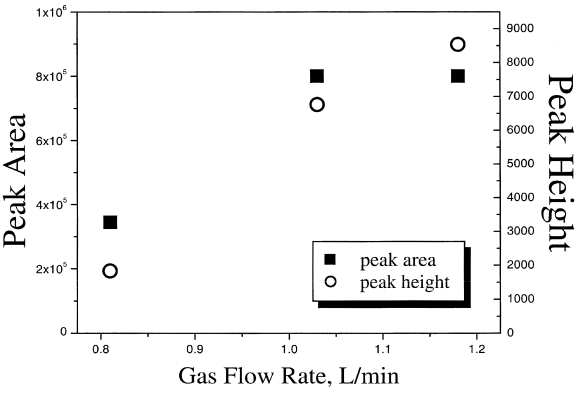

Fig. 3. Cu emission intensity versus carrier gas flow-rate for the outer electrode CE–ICP configuration. CE voltage was not applied.

(Fig. 3). The trend of intensity versus gas flow-rate is opposite to that of elution time. The selection of carrier gas flow-rate in the following sections is a compromise of good sensitivity and long elution time.

3.3. Peak broadening due to carrier gas flow

As the gas flow-rate increases, the peak width measured in time units decreases (Fig. 4a). A fixed volume of 1.6 μl of Cu^{2+} solution was injected into the CE capillary as described above. Again, no CE voltage was applied. The sample plug was eluted by applying a carrier gas flow.

The apparent reduction in peak width versus gas flow-rate is a result of faster solution flow-rate inside the capillary at higher gas flow-rate (Fig. 4a). Peak width measured in physical length of the eluted sample plug is a better gauge of the peak broadening effects due to the carrier gas flow (Fig. 4b).

Since hydrodynamic sample injection was used, the initial length and volume of the sample is determined by the injection pressure and the duration of pressure application. The length of the sample was measured experimentally using a microscope by injecting a concentrated solution of $KMnO_4$ into the capillary. For injection gas pressure of 5 p.s.i. and duration of 20 s, the initial sample length was ~20 cm. The length of the eluted sample plug is esti-

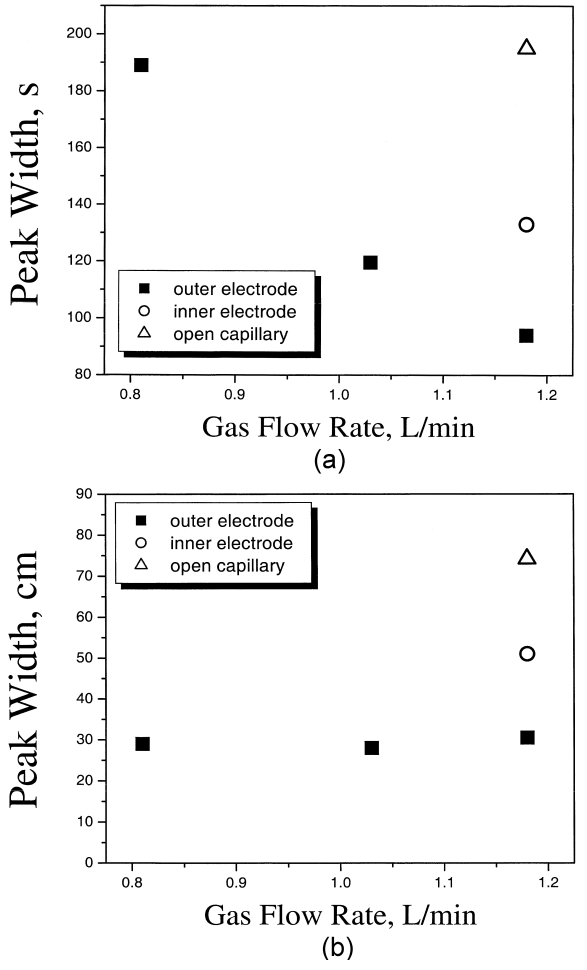

Fig. 4. Peak width of the Cu peak versus carrier gas flow-rate for the outer electrode CE–ICP configuration. CE voltage was not applied. (a) Peak width in time, (b) physical length of the eluted sample plug. Peak widths of the inner electrode and open capillary configurations at gas flow-rate of 1.18 l/min are shown for comparison.

mated from the elution time and the width (at 10% peak height above the baseline) of the eluted peak:

$$\text{sample length (cm)} = \frac{\text{peak width (s)}}{\text{elution time (s)}} \cdot \left[\text{capillary length (cm)} - \frac{\text{initial length (cm)}}{2} \right]$$

For the outer electrode configuration, the length of the eluted sample plug is close to the injected sample length. The eluted peak is approximately trapezoidal in shape, with baseline width of ~30 cm and half width of ~20 cm (Fig. 4b).

For comparison, the peak width for the inner electrode and open capillary configurations at a gas flow-rate of 1.18 l/min are also shown in Fig. 4a and b. With a Pt wire wrapped across the exit end of the CE capillary, the opening of the capillary is partially blocked. The solution flow-rate is reduced (Fig. 2). Importantly, the peak width is also reduced using the outer electrode configuration for the same gas flow-rate (Fig. 4a and b). The restricted opening of the outer electrode configuration reduces peak broadening.

3.4. Stability of electrical connection

The platinum electrode was placed outside the end of the CE capillary. There is a possibility of poor electrical contact between the CE electrolyte solution and the electrode. The electrophoretic current will then become unstable. The electrophoretic current during a CE–ICP run with 0.02 *M* sodium acetate electrolyte solution is shown in Fig. 5. The CE voltage was 15.0 kV; capillary length was 150 cm and diameter was 100 μm; carrier gas flow-rate was 0.81 l/min. The current drops slightly during the first 20 s and remains constant afterward. The initial drop in the current is probably due to the capacitive current charging up the CE capillary. However, there is no fluctuation in the current due to poor electrical contact during a CE run over the 10-min period.

The electrophoretic current of a CE run for a sample solution of 50 μg/ml each of Cr^{3+} and $Cr_2O_7^{2-}$ is also shown in Fig. 5. Sample length was ~20 cm. The same buffer of 0.02 *M* sodium acetate was used. The current is lower during the first 400 s because of lower conductivity of the sample plug. At the end of the CE run, the sample plug was eluted out of the capillary and the current returned to the same level as the buffer electrolyte.

Stable electrophoretic current was observed for carrier gas flow-rates of 0.4 to 1.5 l/min.

3.5. CE separation of small ions

A typical electropherogram for the separation of

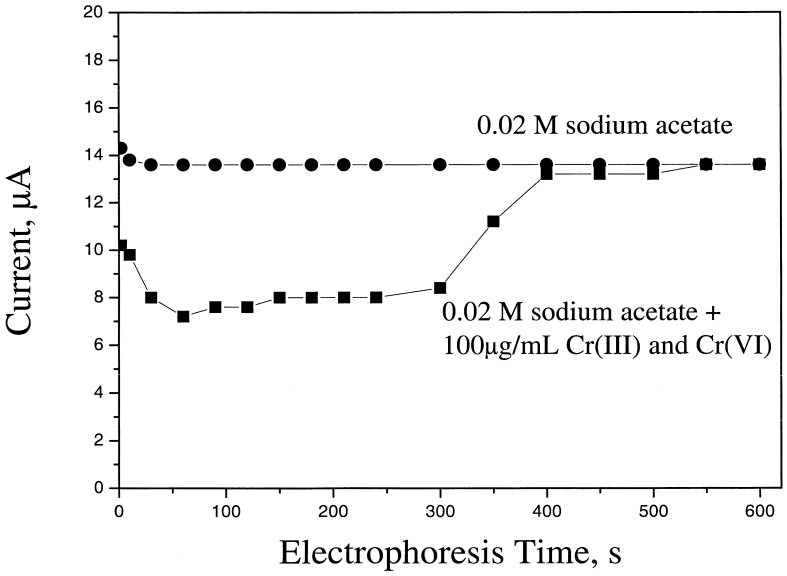

Fig. 5. Electrophoretic current versus electrophoresis time.

Cr(III) and Cr(VI) species using CE–ICP-AES is shown in Fig. 6. The sample solution is the same as above: 50 μg/ml each of Cr^{3+} and $Cr_2O_7^{2-}$; sample length was ~10 cm; total capillary length was 150 cm. The CE voltage was 15 kV. The carrier gas flow-rate was 0.81 l/min. The lower peak height of Cr^{3+} versus $Cr_2O_7^{2-}$ is probably because the highly charged Cr^{3+} cation is easily trapped by the electric double layer [25]. The areas of the peaks, however, are approximately equal.

In addition to carrier gas flow-rate, the diameter of the CE capillary also influences the CE resolution. A smaller inner diameter of the CE capillary will result in a lower electrolyte flow-rate and thus a higher resolution. Electropherograms for the separation of Cu^{2+} and Cu-$EDTA^{2-}$ are shown in Fig. 7. CE operating parameters similar to previous section were used: CE voltage was 15.0 kV; capillary length 135 cm. Total Cu^{2+} concentration was 100 μg/ml; Cu^{2+} to EDTA mol ratio was 2:1. The resolution using a capillary of inner diameter 75 μm is higher than that of a capillary of inner diameter 100 μm (Fig. 7). The capillaries have the same outer diameter of 363 μm. The same carrier gas flow-rate of 0.7 l/min was also used for both configurations. Therefore, the configuration of the nebulizer, and thus the gas flow pattern, is the same for both capillaries. The peak area for the smaller capillary is approximately 50% of that of the larger capillary because the ratio of the cross-sectional areas and thus the injected sample volume is 1:2 for the capillaries.

3.6. Effectiveness of the custom cooling system

Olesik et al. discussed the sources of band broadening for CE–ICP in detail [6]. A major source of band broadening is the increase in diffusion rate of the analyte in the capillary due to Joule heating. For CE–ICP, a section of the CE capillary extending from the CE to the ICP spectrometer is usually exposed to the atmosphere and its temperature is not regulated. Peak broadening due to Joule heating can be severe, especially for capillaries of large inner diameter.

In this study, a simple, low-cost cooling system using a peristaltic pump to circulate water around the capillary for the CE capillary has been developed. The cooling system reduces peak broadening due to Joule heating effectively (Fig. 8). As the potential

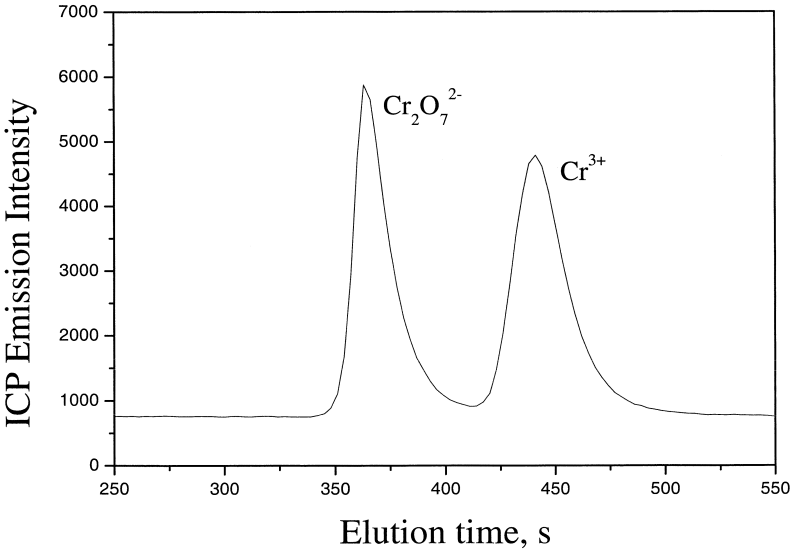

Fig. 6. Electropherogram of Cr(III) and Cr(VI) for CE–ICP-AES. CE voltage = 15 kV; polarity of electrode at the CE–ICP interface is positive relative to the electrode at the inlet.

difference increases, electrophoretic current and thus Joule heating increases. The heat energy carried away by the flow of electrolyte solution can be estimated from the solution flow-rate. Heat loss via solution flow is small despite of the increased flow-rate by the carrier gas flow. If the capillary is

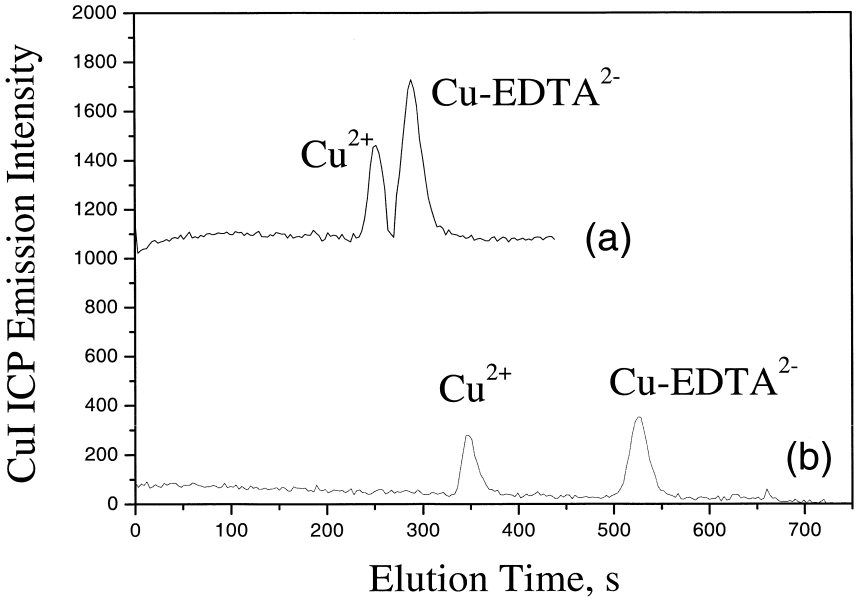

Fig. 7. Electropherogram of Cu^{2+} and Cu-$EDTA^{2-}$ using capillaries of inner diameter of (a) 100 μm and (b) 75 μm. Curve (a) is offset by 1000 for clarity. CE voltage = 15 kV; polarity of electrode at the CE–ICP interface is negative relative to the electrode at the inlet.

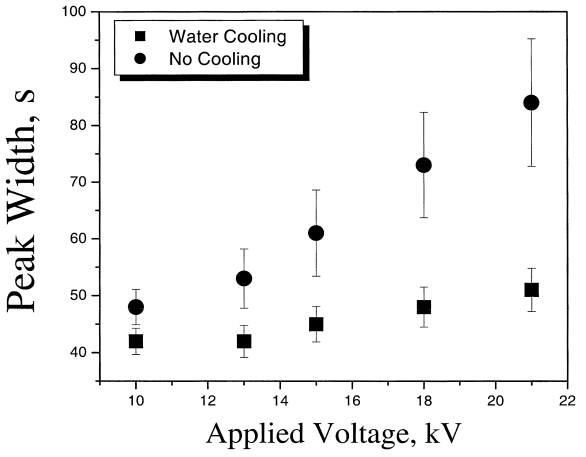

Fig. 8. CE–ICP peak width of Cu-EDTA^{2-} versus electrophoretic voltage.

exposed to the atmosphere without active cooling, the temperature of capillary increases significantly. Joule heating of the electrolyte solution increases the diffusion rate of the analyte and the peak width increases with applied voltage (Fig. 8). The reproducibility of peak width also reduces with heating; relative standard deviations (RSDs) of peak width were 4% and 10% with and without cooling, respectively.

3.7. Analytical figures of merit

The RSDs in ICP emission intensity measurements of Mn (peak height and peak area) for three successive injections of $KMnO_4$ with no electric field applied are 1.5 and 1.8%, respectively (Table 1). The RSD represents the precision of sample injection as well as the nebulization and transport processes of the aerosol. With the application of an electric field for the separation of the $Cr^{3+}/Cr_2O_7^{2-}$ and Cu^{2+}/Cu-EDTA^{2-} pairs, the RSD is approximately 3 to 4%.

Table 1
Reproducibility of ICP emission intensity for CE–ICP-AES[a]

Metal species	Applied voltage (kV)	RSD (%) ($n=3$)	
		Peak height	Peak area
MnO_4^-	0	1.5	1.8
Cr^{3+}	15	3.2	2.5
$Cr_2O_7^{2-}$	15	2.8	1.7
Cu^{2+}	15	3.5	3.3
Cu-EDTA^{2-}	15	3.7	2.5

[a] CE capillary inner diameter = 100 μm; capillary length = 150 cm; sampling length = 10 cm. Concentration of MnO_4^- = 100 μg/ml; concentration of other metal species = 50 μg/ml. Buffer solution = 0.02 *M* sodium acetate, pH 5. Carrier gas flow-rate = 0.81 l/min. Emission lines: Mn II 260.6 nm, Cr II 266.7 nm, Cu I 324.7 nm.

Table 2
Detection limits of CE–ICP-AES[a]

Metal species	Detection limit (ng/ml)
Cr^{3+}	1.5
$Cr_2O_7^{2-}$	1.8
Cu^{2+}	4.6
Cu-EDTA^{2-}	2.6

[a] Applied voltage = 15 kV; standard solution concentration = 50 μg/ml; other experimental conditions as in Table 1.

Detection limits (3σ) based on peak area are 2 to 5 ng/ml (Table 2). The detection limits are calculated using standard deviation of the background before the CE–ICP peak [26].

The reproducibility of the system is further estimated by disassembling and re-assembling the CE–ICP interface between CE runs. RSD of ICP emission intensity and elution time are less than 4% for Cu^{2+}/Cu-EDTA^{2-} separation.

4. Conclusions

A CE–ICP interface based on a concentric nebulizer has been developed. The interface is relatively simple to build and is easy to set up to couple a commercial capillary electrophoresis to the ICP spectrometer. Initial results show that the CE–ICP set-up provides adequate resolution and sensitivity for the separation and detection of $Cr^{3+}/Cr_2O_7^{2-}$ and Cu^{2+}/Cu-EDTA^{2-}.

A cooling technique using a peristaltic pump to circulate water over the CE capillary was first used in CE–ICP. Cooling reduces peak broadening and improves the reproducibility of CE–ICP measurements.

Acknowledgements

This research work is financed by a CRCG research grant and by the Department of Chemistry of the University of Hong Kong.

References

[1] P. Camilleri (Ed.), Capillary Electrophoresis – Theory and Practice, 2nd ed., CRC Press, Boca Raton, FL, 1998.
[2] Z. Deyl, I. Mikšík, F. Tagliaro, Forensic Sci. Int. 92 (1998) 89.
[3] A.R. Timerbaev, E. Dabek-Zlotorzynska, M.A.G.T. van den Hoop, Analyst 124 (1999) 811.
[4] Y. Xu, Anal. Chem. 71 (1999) 309R.
[5] E. Dabek-Zlotorzynska, E.P.C. Lai, A.R. Timerbaev, Anal. Chim. Acta 359 (1998) 1.
[6] J.W. Olesik, J.A. Kinzer, S.V. Olesik, Anal. Chem. 67 (1995) 1.
[7] Q. Lu, S.M. Bird, R.M. Barnes, Anal. Chem. 67 (1995) 2949.
[8] M.J. Tomlinson, L. Lin, J.A. Caruso, Analyst 120 (1995) 583.
[9] Y. Liu, V. Lopez-Avila, J.J. Zhu, D.R. Wiederin, W.F. Beckert, Anal. Chem. 67 (1995) 2020.
[10] J.A. Kinzer, J.W. Olesik, S.V. Olesik, Anal. Chem. 68 (1996) 3250.
[11] Q. Lu, R.M. Barnes, Microchem. J. 54 (1996) 129.
[12] B. Michalke, P. Schramel, Fresenius J. Anal. Chem. 357 (1997) 594.
[13] E. Mei, H. Ichihashi, W. Gu, S. Yamasaki, Anal. Chem. 69 (1997) 2187.
[14] M.L. Magnuson, J.T. Creed, C.A. Brockhoff, J. Anal. Atom. Spectrom. 12 (1997) 689.
[15] A. Tangen, R. Trones, T. Greiborokk, W. Lund, J. Anal. Atom. Spectrom. 12 (1997) 667.
[16] S.D. Lofthouse, G.M. Greenway, S.C. Stephen, J. Anal. Atom. Spectrom. 12 (1997) 1373.
[17] S. Lusting, B. Michalk, W. Beck, P. Schramel, Fresenius J. Anal. Chem. 360 (1998) 18.
[18] K.A. Taylor, B.L. Sharp, D.J. Lewis, H.M. Crews, J. Anal. Atom. Spectrom. 13 (1998) 1095.
[19] K.L. Sutton, C. B'Hymer, J.A. Caruso, J. Anal. Atom. Spectrom. 13 (1998) 885.
[20] M. Vahid, N.J. Miller-Ihli, Analyst 123 (1998) 803.
[21] M.V. Holderbeke, Y. Zhao, F. Vanhaecke, L. Moens, R. Dams, P. Sandra, J. Anal. Atom. Spectrom. 14 (1999) 229.
[22] X.D. Tian, Z.X. Zhuang, B. Chen, X.R. Wang, Analyst 123 (1998) 899.
[23] R.M. Barnes, Fresenius J. Anal. Chem. 361 (1998) 246.
[24] Y.Y. Chan, W.T. Chan, J. Chromatogr. A 853 (1999) 141.
[25] M.R. Schure, A.M. Lenhoff, Anal. Chem. 65 (1993) 3024.
[26] R. Kuhn, S. Hoffstetter-Kuhn, in: Capillary Electrophoresis – Principles and Practice, Springer-Verlag, Berlin, 1993, p. 111.